Comparison of the Dispersion Properties of Several Low-Dispersion Finite-Difference Time-Domain Algorithms

Kurt L. Shlager, *Senior Member, IEEE,* and John B. Schneider

***Abstract*—A comparison of the accuracy of several low-dispersion finite-difference time-domain (FDTD) schemes in two dimensions is presented. Each algorithm is briefly reviewed and its FDTD update equations presented. The dispersion relation of each FDTD algorithm is also given. The accuracy of each FDTD scheme is compared via direct evaluation of the dispersion relation. Results are presented showing the dispersion errors of each algorithm as a function of propagation angle and cell size. Tables are shown that present for each algorithm the optimal Courant number at a specified discretization as well as the number of floating point operations needed to update each cell (three fields) at each time step. The advantages and disadvantages of each algorithm are briefly discussed. While some schemes are more wideband than others, almost all provide substantial improvement in the dispersion errors compared with the classical Yee FDTD algorithm.**

***Index Terms*—Finite-difference time-domain (FDTD) methods, multiresolution time domain (MRTD), numerical dispersion.**

I. Introduction

FOR ELECTRICALLY large problems, the numerical dispersion inherent in the classical Yee finite-difference time-domain (FDTD) algorithm can introduce significant errors. Over the past ten years, there have been several FDTD schemes published with the goal of reducing dispersion errors. In 1993, Shlager *et al.* [1] compared the dispersion errors of several FDTD algorithms: Yee's FDTD algorithm [2]; Fang's second-order in time fourth-order in space (2,4) algorithm FDTD scheme [3]; Fang's fourth-order in time, fourth-order in space (4,4) FDTD scheme [3]; Bi *et al.* 's collocated FDTD algorithm [4]; and Chen *et al.* 's transmission line matrix (TLM)-FDTD algorithm [5]. Since then, several new low-dispersion FDTD schemes have been published.

Nehrbass, Jetvić, and Lee (NJL) presented a simple reduced-dispersion algorithm that adjusted the numerical velocity of the wave in the FDTD grid such that the dispersion error was zero when averaged over all angles [6]. The NJL scheme is similar to the "dispersion-optimized" scheme previously put forward by Taflove [7, pp. 102–105]. Starting from the integral form of Maxwell's equations in conjunction with Fang's (2,4) FDTD scheme, Hadi and Piket-May derived a modified second-order in time, fourth-order in space, M(2,4), FDTD scheme [8]. In the M(2,4) scheme, the global dispersion error is minimized over all propagation angles. Recently, Turkel and Yefet presented an implicit second-order in time, fourth-order in space Ty(2,4) FDTD algorithm [9], [10]. Their algorithm uses implicit spatial derivatives, while maintaining the standard Yee leapfrog timestepping. Meanwhile, Cole utilized nonstandard finite differences to derive a Yee-like FDTD algorithm with low dispersion [11]. Forgy developed an algorithm that uses both the Yee grid and the Bi collocated grid. Since these grids have complementary dispersion characteristics, Forgy was able to combine them in such a way as to eliminate nearly all dispersion errors at a design frequency [12]–[14]. In 1996, Krumpholz and Katehi proposed the multiresolution time-domain (MRTD) method [15]. In their scheme, field components are expanded in scaling and wavelet functions with respect to space. Pulse functions are used as basis and testing functions with respect to time. Krumpholz and Katehi chose to work primarily with the cubic spline Battle-Lemarie (B–L) scaling and wavelet functions, although other scaling and wavelet functions are possible. Instead of the B–L scaling functions, Goverdhanam *et al.* [16]–[18] and Fujii and Hoefer [19], [20] used Haar scaling functions, which have much more compact support. Recently, Cheong *et al.* [21] used the compactly supported Daubechies scaling functions to avoid the nonlocalization of the B–L scaling functions.

In [1], the optimal dispersion characteristics of the Fang(2,4) scheme were mistakenly identified as occurring at the Courant stability limit. For this reason, the Fang (2,4) scheme is re-evaluated in this paper. In addition, the dispersion relation of the NJL reduced-dispersion scheme, Hadi and Piket-May's M(2,4) scheme, Turkel and Yefet's Ty (2,4) implicit scheme, Cole's nonstandard scheme, Forgy's isotropic scheme, and the MRTD schemes mentioned previously are all presented. Other low-dispersion methods have been introduced which are not considered here. Some of these schemes, such as those presented by Omick and Castillo [22], Liu [23], Fujii and Hoefer [24], [25], and Dogaru and Carin [26], may posses certain properties that are comparable to, or even superior to, those of some of the algorithms considered here (though certainly no algorithm is universally superior to the others). Since time and space dictate limiting the number of algorithms reported, we have chosen algorithms based on the interest in the algorithm and/or the perceived benefits it has relative to others.

After a short review of dispersion error, each of these FDTD algorithms is reviewed in two dimensions and its two-dimensional (2-D) dispersion relation presented (Sections III–IX). Al-

Manuscript received March 9, 2001; revised January 9, 2002. This work was supported by the Office of Naval Research under Code 321OA.

K. L. Shlager is with Lockheed-Martin, Sunnyvale, CA 94089 USA (e-mail: kurt.shlager@lmco.com).

J. B. Schneider is with the School of Electrical Engineering and Computer Science, Washington State University, Pullman, WA 99164-2752 USA (e-mail: schneidj@eecs.wsu.edu).

Digital Object Identifier 10.1109/TAP.2003.808532

though the results presented here are limited to those obtained from the 2-D dispersion analysis, where appropriate the three-dimensional (3-D) behavior of each algorithm is also briefly addressed.

To facilitate comparison of the computational effort and size of the spatial stencils, we also provide the update equations for each scheme. Similar FDTD schemes are compared against one another. Results are presented showing the dispersion errors of each algorithm as a function of propagation angle and cell size. Since each of these schemes either permits or requires optimization at a particular frequency, curves are presented showing their performance when optimized at ten cells per wavelength. In Section X, further comparisons of the dispersion algorithms are made. The optimal Courant number to be used for each algorithm is given as well as the number of floating point operations needed to update each cell (three fields) at each time step. In addition, a figure is presented comparing the dispersion errors for all schemes when each scheme is optimized at 30 cells per wavelength (CPW). Finally, a summary of the advantages and disadvantages of each algorithm is presented.

II. Review of FDTD Dispersion

The dispersion characteristics of an FDTD algorithm are typically derived by assuming a time harmonic solution to the discretized form of Maxwell's equations for an isotropic, homogeneous, linear, and lossless medium. The dispersion relations describe the phase velocity of an electromagnetic plane wave propagating in the grid and can be used to determine the dispersion error per numerical wavelength $\tilde{\lambda}$. This error is a function of the angle of propagation of the plane wave, the number of CPW, and the Courant number, which is given by $S = c\Delta t/\delta$, where c is the speed of light, Δt is the time step, and δ is the spatial increment. Throughout this paper, we assume a 2-D uniform grid with spatial increments $\Delta x = \Delta y = \delta$.

For reference, we include the Yee update equations for the lossless 2-D transverse magnetic (TM_z) case

$$E_z\Big|_{i,j}^{n+1} = E_z\Big|_{i,j}^{n} + \frac{\Delta t}{\epsilon\delta}\left(H_y\Big|_{i+1/2,j}^{n+1/2} - H_y\Big|_{i-1/2,j}^{n+1/2} - H_x\Big|_{i,j+1/2}^{n+1/2} + H_x\Big|_{i,j-1/2}^{n+1/2}\right) \quad (1)$$

$$H_x\Big|_{i,j+1/2}^{n+1/2} = H_x\Big|_{i,j+1/2}^{n-1/2} - \frac{\Delta t}{\mu\delta}\left(E_z\Big|_{i,j+1}^{n} - E_z\Big|_{i,j}^{n}\right) \quad (2)$$

$$H_y\Big|_{i+1/2,j}^{n+1/2} = H_y\Big|_{i+1/2,j}^{n-1/2} + \frac{\Delta t}{\mu\delta}\left(E_z\Big|_{i+1,j}^{n} - E_z\Big|_{i,j}^{n}\right) \quad (3)$$

where ϵ and μ are the permittivity and permeability of the medium. In two dimensions, the algorithm has a Courant stability relation given by

$$c\Delta t \le \frac{1}{\sqrt{\left(\frac{1}{\Delta x}\right)^2 + \left(\frac{1}{\Delta y}\right)^2}}. \quad (4)$$

For a uniform grid, (4) reduces to $S \le 1/\sqrt{2}$.

The dispersion relation is given by

$$\left(\frac{\delta}{c\Delta t}\right)^2 \sin^2\left(\frac{\omega\Delta t}{2}\right) = \sin^2\left(\frac{\tilde{k}_x\delta}{2}\right) + \sin^2\left(\frac{\tilde{k}_y\delta}{2}\right) \quad (5)$$

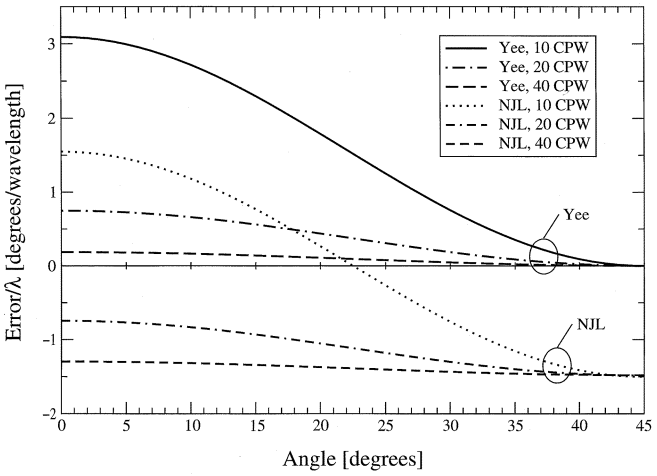

Fig. 1. Error versus propagation angle for the Yee and NJL schemes for discretizations of 10, 20, and 40 CPW. For the NJL scheme, the speed of light has been optimized for 10 CPW.

where $\tilde{k}_x$ and $\tilde{k}_y$ are the x and y components of the numerical wavenumber, respectively, and ω is the angular frequency. For error analysis it is more convenient to write (5) in the following form:

$$\frac{1}{S^2}\sin^2\left(\frac{\pi}{N_\lambda}S\right) = \sin^2\left(\frac{\pi}{N_\lambda}\frac{\lambda}{\tilde{\lambda}}\cos\phi\right) + \sin^2\left(\frac{\pi}{N_\lambda}\frac{\lambda}{\tilde{\lambda}}\sin\phi\right) \quad (6)$$

where N_λ is the CPW (note that CPW is the number of cells per the exact wavelength, i.e., CPW $= \lambda/\delta$ and is not the number of cells per the numeric wavelength), ϕ is the direction of propagation with 0° corresponding to propagation along a grid axis, and $\lambda/\tilde{\lambda}$ is the ratio of the exact to numeric wavenumber. The dispersion error per wavelength can be obtained through the relation

$$\psi_{\rm err} = 360^\circ\left(\frac{\lambda}{\tilde{\lambda}} - 1\right). \quad (7)$$

Throughout the paper, a simple bisection approach is used to obtain the ratio $\lambda/\tilde{\lambda}$ from the appropriate dispersion relation.

The Yee FDTD algorithm is second-order accurate. If the cell size is decreased by a factor m, the error decreases by m^2. This is illustrated in Figs. 1 and 2. Fig. 1 shows the error versus the propagation angle for discretizations of 10, 20, and 40 CPW. For these discretizations, and, in fact, for all practical discretizations, waves propagate slower than the speed of light [7], [27], [28]. At the 2-D Courant limit, which minimizes dispersion and is used here, there is no dispersion error for propagation along the cell diagonals ($\phi = 45°$, 135°, 225°, or 315°) and the error is maximum along the grid axes ($\phi = 0°$, 90°, 180°, or 270°). The dispersion relation is periodic and symmetric about the grid diagonals so that only angles between 0°–45° are shown. Fig. 2 shows the maximum dispersion error over all angles versus CPW and further illustrates the second-order behavior of the Yee algorithm.

There are several ways to analyze, interpret, and plot dispersion error. Ultimately, individuals must decide if an algorithm provides acceptable dispersion for their particular application. From Figs. 1 and 2 and the Yee dispersion relation, clearly the

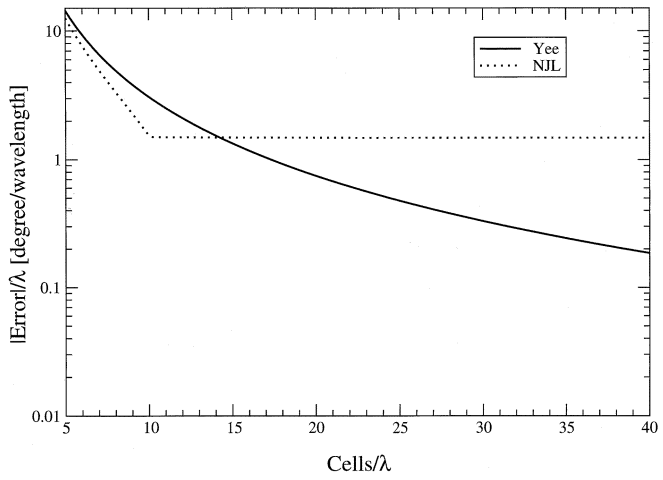

Fig. 2. Maximum error versus CPW for the Yee and NJL schemes. For the NJL scheme, the speed of light has been optimized for 10 CPW.

dispersion error is larger for coarse discretizations (short wavelengths) than it is for fine discretizations (long wavelengths). The algorithms we describe in the following sections all attempt to provide dispersion characteristics that are superior to that of the Yee algorithm. However, this does not necessarily equate to providing improved performance over all discretizations. Since the Yee algorithm is worse at coarse discretizations than at fine ones, coarse discretizations are typically where one wants to realize the largest reduction in error. At fine discretizations, the Yee algorithm performs well and further improvements might be considered overkill. In fact, an argument can be made that a linear *increase* in dispersion errors for increasing cell density is acceptable.

Consider an object with a characteristic length of L corresponding to $N_{\max}$ wavelengths at the highest frequency of interest. Assume that we require the total phase error be less than ζ° for propagation over the distance L, i.e., there should be no more phase error than $\zeta/N_{\max}{}^\circ$ per wavelength of propagation. For the Yee algorithm, the discretization needed to achieve this level of accuracy is straightforward to determine. For frequencies less than the maximum, the electrical length of the object is correspondingly reduced. For example, if the frequency is halved, the electrical length is also halved so that the object appears $N_{\max}/2$ wavelengths long. For this same reduction in frequency, the per-wavelength dispersion error in the Yee algorithm is reduced by a factor of four resulting in a total phase error for propagation over the distance L of $\zeta/8$. If a total phase error of ζ° was deemed to be acceptable at the maximum frequency, the Yee algorithm will perform much better than that at lower frequencies, i.e., the phase error will be less than ζ and exhibit second-order reduction as the frequency is decreased. Now, consider a hypothetical algorithm where the phase error increases linearly with decreasing frequency. For that algorithm, the total phase error associated with propagation a distance L would be ζ^{circ} for all frequencies. The error at all frequencies would be right at the acceptable level (no better, no worse). As we shall see, many of the new schemes do (or can do) much better than the Yee algorithm at coarse discretizations. This improvement sometimes comes at the price of doing worse than the Yee algorithm at lower frequencies. Given the preceding arguments, this should not necessarily be considered an undesirable trait.

Finally, it is noted that, as shown in [1], the dispersion characteristics of the Yee algorithm are slightly worse in three dimensions than two dimensions due to the decreased Courant stability limit, i.e., $S \leq 1/\sqrt{3}$, with the maximum dispersion error still along the coordinate axes.

III. NJL FDTD Algorithm

In [6], Nehrbass, Jevtić, and Lee modified the FDTD update coefficients so that the numerical phase velocity for a given discretization was equal to the speed of light at a propagation angle of $\phi = 22.5^\circ$, i.e., halfway between angles corresponding to the maximum and minimum dispersion errors in the Yee algorithm. Their algorithm has a wave velocity which is slower than the speed of light for angles $0^\circ < \phi < 22.5^\circ$, and a wave velocity which is faster than light for angles $22.5^\circ < \phi < 45^\circ$. The dispersion error averaged over all angles is zero. Nehrbass *et al.* prescribed adjustments that can be used in two or three dimensions. However, the adjustment of the numerical speed of light to correct for dispersion error was previously put forward by Taflove [7] who used such a scheme to obtain zero dispersion errors along the grid diagonals when using a less-than-optimum Courant number. The NJL dispersion relation is given by

$$\frac{1}{v_r^2 S^2}\sin^2\left(\frac{\pi}{N_\lambda}S\right) = \sin^2\left(\frac{\pi}{N_\lambda}\frac{\lambda}{\tilde{\lambda}}\cos\phi\right) + \sin^2\left(\frac{\pi}{N_\lambda}\frac{\lambda}{\tilde{\lambda}}\sin\phi\right) \quad (8)$$

where v_r is the speed of light in the grid and is given by

$$v_r = \frac{\sin\left(\frac{\pi}{N'_\lambda}S\right)}{S\sqrt{\sin^2\left(\frac{\pi}{N'_\lambda}\cos\frac{\pi}{8}\right) + \sin^2\left(\frac{\pi}{N'_\lambda}\sin\frac{\pi}{8}\right)}} \quad (9)$$

and N'_λ is the cells per wavelength at the frequency at which the average error is zero, i.e., the "design frequency." The dispersion relation (8) holds for all N_λ but in an NJL FDTD simulation, the design frequency, and, hence, N'_λ is fixed *a priori*.

The FDTD update equations for the NJL scheme are identical to the Yee update equations except for the adjustment of the material parameters to yield a speed of light of v_r given in (9). The NJL scheme prescribes the parameters needed to realize zero error when averaged over all angles. However, in applications where the propagation is principally in a known direction, it may be preferable to adjust the parameters so that the phase velocity is correct for that direction (see, for example, [7, p. 125]).

The NJL scheme halves the maximum error, compared with the Yee scheme, at the design frequency. At lower frequencies (i.e., longer wavelengths or finer discretizations) the maximum error is nearly identical to that at the design frequency. To illustrate why this occurs, Fig. 1 shows the error in the NJL scheme for discretizations of 10, 20, and 40 CPW. The speed of light has been adjusted so that the average error at 10 CPW is zero. This adjustment essentially shifts the Yee curves so that the 10 CPW curve has zero mean. However, at finer discretizations this offset is still present. This is also clearly seen in Fig. 2, where the maximum dispersion error over all angles is plotted as a function of the discretization. So, unlike the Yee algorithm which con-

TABLE I
FLOATING POINT OPERATIONS PER CELL AND OPTIMUM COURANT NUMBER AT 10 AND 30 Cells/λ. FOR THE M(2,4) SCHEME, K_1 AND K_2 ARE AS SPECIFIED IN [8]. FOR THE FANG(2,4), TY(2,4), AND BATTLE-LEMARIE AND DAUBECHIES MRTD SCHEMES, THE COURANT NUMBERS WERE DETERMINED EMPIRICALLY TO MINIMIZE MAXIMUM ERROR AT EITHER 10 OR 30 Cells/λ

	Method	FLOPs	Optimum Courant Number at 10 cells/λ	30 cells/λ
	Yee	11	$\frac{1}{\sqrt{2}} = 0.7071$	$\frac{1}{\sqrt{2}}$
	NJL	11	$\approx \frac{1}{\sqrt{2}} = 0.7071$	$\approx \frac{1}{\sqrt{2}}$
	Fang (2,4)	22	0.166	.0565
	M24	31	$\frac{3}{\sqrt{2(3-4K_1)(3-4K_1-2K_2)}} = 0.6257$	0.6296
	Ty(2,4)	32	0.1323	0.0441
	Forgy	20	$\frac{\sqrt{3}}{2} = 0.8660$	$\frac{\sqrt{3}}{2}$
	Cole	23	$\frac{3\sin^{-1}(3/4)}{\pi} = 0.8098$	$\frac{3\sin^{-1}(3/4)}{\pi}$
MRTD	Battle-Lemarie	144	0.2575	0.1414
MRTD	Daubechies	48	0.033	0.0141
MRTD	Haar	11	$\frac{1}{\sqrt{2}} = 0.7071$	$\frac{1}{\sqrt{2}}$

verges to zero error in the limit of vanishing discretization, the NJL scheme converges to the offset value needed to adjust the 10 CPW curve to zero mean. These results may appear at odds with the results presented in [6]. However, these results can be reconciled by keeping in mind that the simulation present in [6] did not pick out the maximum error for a given discretization. Furthermore, the angle of propagation in their waveguide simulation was a function of frequency so that they obtained results at different angles for different frequencies.

There is essentially no additional computational cost associated with the NJL scheme compared to the Yee scheme; however, the Courant number must be reduced slightly from that of the Yee limit to prevent numerical instabilities. The results shown in Figs. 1 and 2 used a Courant number of $1/\sqrt{2}$ for both algorithms since the slight amount of reduction required to obtain stable results for the NJL scheme has almost no effect on these results.

The NJL adjustments to the Yee algorithm in 3-D result in behavior similar to the 2-D case with the maximum dispersion error halved at the design frequency and nearly constant error at all frequencies lower than the design frequency.

IV. FANG(2,4) FDTD ALGORITHM

The first higher-order FDTD scheme was presented by Fang in 1989 [3]. He used fourth-order centered spatial differences and timestepping based on second-order centered differences. Such expressions can be obtained via Taylor series expansions and lead to increased spatial stencils in both the electric and magnetic fields compared to the Yee algorithm. As shown in Table I, these larger stencils require twice the number of floating point operations (FLOPs) per cell and per time step as the Yee algorithm. The TM_z Fang(2,4) update equations are given by

$$\begin{aligned} E_z\big|_{i,j}^{n+1} =& E_z\big|_{i,j}^{n} + \frac{9\Delta t}{8\epsilon\delta}\left(H_y\Big|_{i+1/2,j}^{n+1/2} - H_y\Big|_{i-1/2,j}^{n+1/2} \right. \\ & \left. - H_x\Big|_{i,j+1/2}^{n+1/2} + H_x\Big|_{i,j-1/2}^{n+1/2}\right) \\ & - \frac{\Delta t}{24\epsilon\delta}\left(H_y\Big|_{i+3/2,j}^{n+1/2} - H_y\Big|_{i-3/2,j}^{n+1/2} \right. \\ & \left. - H_x\Big|_{i,j+3/2}^{n+1/2} + H_x\Big|_{i,j-3/2}^{n+1/2}\right) \end{aligned} \tag{10}$$

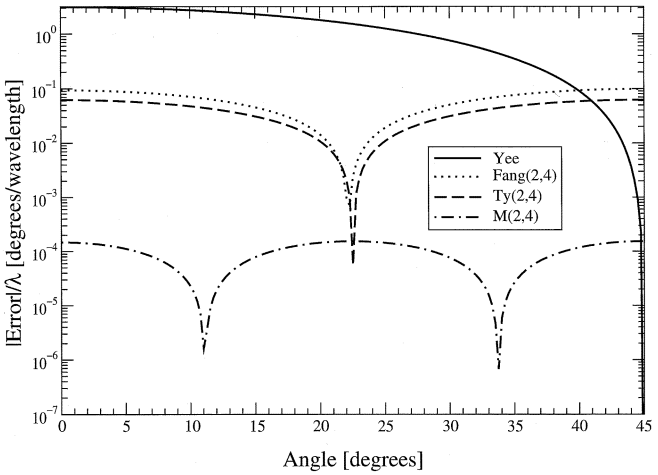

Fig. 3. Error versus propagation angle for the Yee, Fang(2,4), M(2,4), and Ty(2,4) schemes for a discretization of 10 CPW. The higher order schemes have been optimized for 10 CPW.

$$\begin{aligned} H_x\Big|_{i,j+1/2}^{n+1/2} =& H_x\Big|_{i,j+1/2}^{n-1/2} - \frac{9\Delta t}{8\mu\delta}\left(E_z\big|_{i,j+1}^{n} - E_z\big|_{i,j}^{n}\right) \\ & + \frac{\Delta t}{24\mu\delta}\left(E_z\big|_{i,j+2}^{n} - E_z\big|_{i,j-1}^{n}\right) \end{aligned} \tag{11}$$

$$\begin{aligned} H_y\Big|_{i+1/2,j}^{n+1/2} =& H_y\Big|_{i+1/2,j}^{n-1/2} + \frac{9\Delta t}{8\mu\delta}\left(E_z\big|_{i+1,j}^{n} - E_z\big|_{i,j}^{n}\right) \\ & - \frac{\Delta t}{24\mu\delta}\left(E_z\big|_{i+2,j}^{n} - E_z\big|_{i-1,j}^{n}\right). \end{aligned} \tag{12}$$

The dispersion relation for this scheme is given by

$$\begin{aligned} & \frac{1}{S^2}\sin^2\left(\frac{\pi}{N_\lambda}S\right) \\ & = \sin^2\left(\frac{\pi}{N_\lambda}\frac{\lambda}{\tilde{\lambda}}\cos\phi\right)\left(1+\frac{1}{6}\sin^2\left(\frac{\pi}{N_\lambda}\frac{\lambda}{\tilde{\lambda}}\cos\phi\right)\right)^2 \\ & \quad + \sin^2\left(\frac{\pi}{N_\lambda}\frac{\lambda}{\tilde{\lambda}}\sin\phi\right)\left(1+\frac{1}{6}\sin^2\left(\frac{\pi}{N_\lambda}\frac{\lambda}{\tilde{\lambda}}\sin\phi\right)\right)^2. \end{aligned} \tag{13}$$

Fang showed that the 2-D Courant stability limit for this scheme was equal to $6/(7\sqrt{2})$. In [1], the dispersion errors of (13) were evaluated at the Courant stability limit. Upon re-evaluation of the dispersion relation, it was realized that this was not the optimal Courant number for minimum dispersion. Since the method is fourth order in space and second order in time, the time step must be reduced from the Courant limit in order to ensure the errors associated with the temporal discretization are comparable with the spatial errors. Thus, to minimize the dispersion error at 10 CPW, the Courant number should be approximately 0.166 (i.e., $0.235/\sqrt{2}$). Fig. 3 shows the dispersion error versus propagation angle using a Courant number of 0.166. Unlike the Yee algorithm, which has minimum dispersion at 90° intervals, the Fang(2,4) algorithm has minimum dispersion at 45° intervals. Fig. 4 shows the maximum dispersion error versus discretization. It can be seen from the curve that for frequencies with discretizations greater than 10 CPW the scheme has second-order behavior.

In three dimensions, it can be shown that for a discretization of 10 CPW the dispersion error is minimized with a Courant number of approximately 0.155. At this Courant number, the

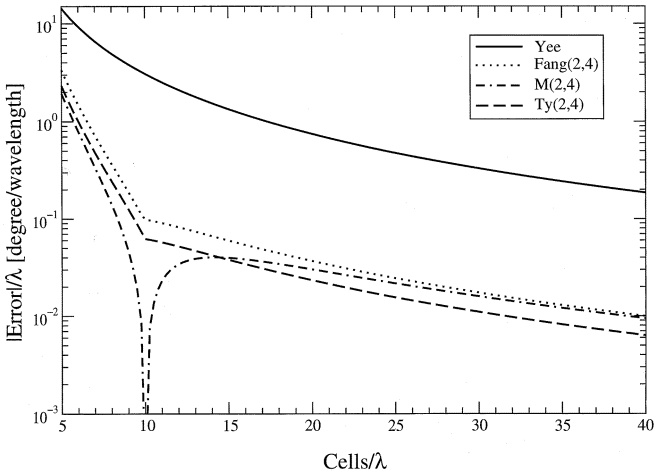

Fig. 4. Maximum error versus CPW for the Yee, Fang(2,4), M(2,4), and Ty(2,4) schemes. The higher order schemes have been optimized for 10 CPW.

dispersion error is equal along the coordinate axes and grid diagonals, with approximately 0.12° of error per wavelength, which is roughly the maximum dispersion error in the 2-D case.

Fang's higher order methods have been the subject of several studies. For example, Young [29] recently presented a similar method that can be generalized to any order. Fang's method, as with all higher-order methods that have extended spatial stencils, requires careful implementation of boundaries which require a discontinuity in the field. Yefet and Petropoulos [30], [31] and Hwang and Cangellaris [32] present schemes to implement boundary conditions that preserve the accuracy of the higher-order method.

V. Hadi and Piket-May M(2,4) FDTD Algorithm

Starting with Fang's (2,4) scheme and utilizing Maxwell's equations in integral form, Hadi and Piket-May showed that Fang's (2,4) update equations could be written as a weighted sum of two different Ampere's law contours [8]. They also showed that by splitting the outer contour into two distinct loops an additional degree of freedom is obtained that provides greater flexibility in reducing the global error. For their scheme, they provided update equation parameters K_1 and K_2 that minimized the dispersion error over all angles at a given design frequency. The updates (10)–(12) are now modified and given by

$$\begin{aligned} E_z\big|_{i,j}^{n+1} =& E_z\big|_{i,j}^{n} + \frac{(1-K_1-K_2)\Delta t}{\epsilon\delta}\Big(H_y\Big|_{i+1/2,j}^{n+1/2} \\ &- H_y\Big|_{i-1/2,j}^{n+1/2} - H_x\Big|_{i,j+1/2}^{n+1/2} + H_x\Big|_{i,j-1/2}^{n+1/2}\Big) \\ &+ \frac{K_1\Delta t}{3\epsilon\delta}\Big(H_y\Big|_{i+3/2,j}^{n+1/2} - H_y\Big|_{i-3/2,j}^{n+1/2} \\ &- H_x\Big|_{i,j+3/2}^{n+1/2} + H_x\Big|_{i,j-3/2}^{n+1/2}\Big) \\ &+ \frac{K_2\Delta t}{6\epsilon\delta}\Big(H_y\Big|_{i+3/2,j-1}^{n+1/2} + H_y\Big|_{i+3/2,j+1}^{n+1/2} \\ &- H_y\Big|_{i-3/2,j-1}^{n+1/2} - H_y\Big|_{i-3/2,j+1}^{n+1/2} \\ &+ H_x\Big|_{i-1,j-3/2}^{n+1/2} + H_x\Big|_{i+1,j-3/2}^{n+1/2} \\ &- H_x\Big|_{i-1,j+3/2}^{n+1/2} - H_x\Big|_{i+1,j+3/2}^{n+1/2}\Big) \end{aligned} \tag{14}$$

$$\begin{aligned} H_x\Big|_{i,j+1/2}^{n+1/2} =& H_x\Big|_{i,j+1/2}^{n-1/2} - \frac{K_1\Delta t}{\mu\delta}\left(E_z\big|_{i,j+1}^{n} - E_z\big|_{i,j}^{n}\right) \\ &+ \frac{(1-K_1)\Delta t}{\mu\delta}\left(E_z\big|_{i,j+2}^{n} - E_z\big|_{i,j-1}^{n}\right) \end{aligned} \tag{15}$$

$$\begin{aligned} H_y\Big|_{i+1/2,j}^{n+1/2} =& H_y\Big|_{i+1/2,j}^{n-1/2} + \frac{K_1\Delta t}{\mu\delta}\left(E_z\big|_{i+1,j}^{n} - E_z\big|_{i,j}^{n}\right) \\ &- \frac{(1-K_1)\Delta t}{\mu\delta}\left(E_z\big|_{i+2,j}^{n} - E_z\big|_{i-1,j}^{n}\right). \end{aligned} \tag{16}$$

As noted in [8], when $K_1 = -1/8$, and $K_2 = 0$, these equations reduce to the Fang(2,4) update equations, while they reduce to the Yee update equations when $K_1 = K_2 = 0$. As shown in Table I, for nonzero K_1 and K_2 the FLOPs per cell and per time step is roughly three times that of the Yee algorithm. Hadi and Piket-May give the optimum values of K_1 and K_2 for CPWs of $5n$ where n is an integer in the range $1 \le n \le 7$. For other discretizations, one must first determine the optimum values via the dispersion relation.

The dispersion relation for this scheme is given by

$$\begin{aligned} &\frac{9}{S^2}\sin^2\left(\frac{\pi}{N_\lambda}S\right) = \\ &\left[K_1\sin\left(\frac{3\pi}{N_\lambda}\frac{\lambda}{\tilde{\lambda}}\cos\phi\right) + 3(1-K_1)\sin\left(\frac{\pi}{N_\lambda}\frac{\lambda}{\tilde{\lambda}}\cos\phi\right)\right] \\ &\left[\sin\left(\frac{3\pi}{N_\lambda}\frac{\lambda}{\tilde{\lambda}}\cos\phi\right)\left(K_1 + K_2\cos\left(\frac{\pi}{N_\lambda}\frac{\lambda}{\tilde{\lambda}}\sin\phi\right)\right)\right. \\ &\left.+3(1-K_1-K_2)\sin\left(\frac{\pi}{N_\lambda}\frac{\lambda}{\tilde{\lambda}}\cos\phi\right)\right] \\ &+\left[K_1\sin\left(\frac{3\pi}{N_\lambda}\frac{\lambda}{\tilde{\lambda}}\sin\phi\right) + 3(1-K_1)\sin\left(\frac{\pi}{N_\lambda}\frac{\lambda}{\tilde{\lambda}}\sin\phi\right)\right] \\ &\left[\sin\left(\frac{3\pi}{N_\lambda}\frac{\lambda}{\tilde{\lambda}}\sin\phi\right)\left(K_1 + K_2\cos\left(\frac{\pi}{N_\lambda}\frac{\lambda}{\tilde{\lambda}}\cos\phi\right)\right)\right. \\ &\left.+3(1-K_1-K_2)\sin\left(\frac{\pi}{N_\lambda}\frac{\lambda}{\tilde{\lambda}}\sin\phi\right)\right]. \end{aligned} \tag{17}$$

At a design frequency of 10 CPW, the optimum values of K_1 and K_2 are -0.116192765 and 0.0734445091, respectively. At this discretization, the optimum Courant number is 0.6257. Plots of the dispersion error versus propagation angle and discretization error, when optimized at 10 CPW, are shown in Figs. 3 and 4, respectively. These figures clearly demonstrate that the dispersion error is greatly reduced at the design frequency. Fig. 3 shows that for most angles, the error has been reduced by more than two orders of magnitude relative to the Fang(2,4) scheme. In addition, the dispersion error is now minimum at 22.5° intervals, instead of the 45° intervals of the Fang scheme. Fig. 4 also shows that at high discretizations—well beyond the design frequency—the dispersion errors asymptotically approach that of the Fang(2,4) scheme.

The implementation of this technique in three dimensions and the treatment of boundary conditions can be found in [33] and [34]. It is noted that the appropriate optimization coefficients for the 3-D case are not given in [33]. Thus, we have not attempted to characterize the dispersion properties of the M(2,4) scheme for the full 3-D algorithm.

VI. Turkel and Yefet's Ty(2,4) Implicit FDTD Algorithm

Turkel and Yefet explored the use of a staggered grid with fourth-order implicit spatial derivatives to reduce the numerical dispersion of Yee's FDTD algorithm [9], [10]. The algorithm is more complex than the explicit FDTD algorithms described previously, since a matrix inversion needs to be computed at each time step for each field component.

The Ty(2,4) update equations are given by

$$E_z\Big|_{i,j}^{n+1} = E_z\Big|_{i,j}^{n} + \frac{\Delta t}{\epsilon\delta}\left(D_x H_y\Big|_{i,j}^{n+1/2} - D_y H_x\Big|_{i,j}^{n+1/2}\right) \tag{18}$$

$$H_x\Big|_{i,j+1/2}^{n+1/2} = H_x\Big|_{i,j+1/2}^{n-1/2} - \frac{\Delta t}{\mu\delta} D_y E_z\Big|_{i,j+1/2}^{n} \tag{19}$$

$$H_y\Big|_{i+1/2,j}^{n+1/2} = H_y\Big|_{i+1/2,j}^{n-1/2} + \frac{\Delta t}{\mu\delta} D_x E_z\Big|_{i+1/2,j}^{n} \tag{20}$$

where the difference operator D_x acting on the field U is defined to be the solution for $(\partial U/\partial x)|_i$ in the following:

$$\frac{U_{i+1/2,j} - U_{i-1/2,j}}{\delta} = \frac{11}{12}\frac{\partial U}{\partial x}\Big|_{i,j} + \frac{1}{24}\left[\frac{\partial U}{\partial x}\Big|_{i+1,j} + \frac{\partial U}{\partial x}\Big|_{i-1,j}\right]. \tag{21}$$

A similar definition holds for D_y. Since $(\partial U/\partial x)|_{i,j}$ depends on $(\partial U/\partial x)|_{i+1,j}$ which, in turn, depends on $U_{i+3/2,j}$ (which depends on $(\partial U/\partial x)|_{i+2,j}$, and so on), the method is implicit—one must solve for all the derivatives simultaneously. However, since each derivative depends only on its neighboring derivatives, the resulting matrix equation is tightly banded and can be solved efficiently.

As shown in Table I, the computational cost of the Ty(2,4) scheme is larger than that of the explicit Fang(2,4) method. In addition, to minimize the numerical dispersion at a design frequency of 10 CPW, the Ty(2,4) method requires the use of a much smaller Courant number than used in the Yee algorithm. At 10 CPW, the optimal Courant number is 0.1323, which is roughly the same as the optimal value for the Fang(2,4) scheme.

The dispersion relation is given by

$$\frac{1}{(12S)^2}\sin^2\left(\frac{\pi}{N_\lambda}S\right) = \left[\frac{\sin\left(\frac{\pi}{N_\lambda}\frac{\lambda}{\lambda}\cos\phi\right)}{11+\cos\left(\frac{2\pi}{N_\lambda}\frac{\lambda}{\lambda}\cos\phi\right)}\right]^2 + \left[\frac{\sin\left(\frac{\pi}{N_\lambda}\frac{\lambda}{\lambda}\sin\phi\right)}{11+\cos\left(\frac{2\pi}{N_\lambda}\frac{\lambda}{\lambda}\sin\phi\right)}\right]^2. \tag{22}$$

The dispersion error versus propagation angle is shown in Fig. 3. The dispersion properties are similar to the Fang(2,4) algorithm with minimum dispersion occurring at 45° intervals. The error is slightly less than that of Fang's. The maximum error versus discretization is shown in Fig. 4. Again, its characteristics are similar to the Fang(2,4) algorithm; its dispersion error behaves as second order for discretizations above the design frequency.

The presentation of this algorithm in [9], [10] was limited to two dimensions. For this reason, we have not attempted to extend the algorithm to three dimensions nor to characterize its dispersion properties in three dimensions. Note that the Ty(2,4) algorithm is similar to the approach suggested by Young *et al.* [35].

VII. Cole's Nonstandard FDTD Algorithm

Employing a different approach to reduce numerical dispersion, Cole developed an FDTD algorithm that employed nonstandard finite differences [11]. The update equations in the TM_z case are given by

$$E_z\Big|_{i,j}^{n+1} = E_z\Big|_{i,j}^{n} + \frac{\Delta t s_\omega(\Delta t)}{\epsilon s_k(\delta)}\Big(H_y\Big|_{i+1/2,j}^{n+1/2} - H_y\Big|_{i-1/2,j}^{n+1/2} - H_x\Big|_{i,j+1/2}^{n+1/2} + H_x\Big|_{i,j-1/2}^{n+1/2}\Big) \tag{23}$$

$$H_x\Big|_{i,j+1/2}^{n+1/2} = H_x\Big|_{i,j+1/2}^{n-1/2} - \frac{\Delta t s_\omega(\Delta t)}{\mu s_k(\delta)}\left(\alpha_0\left(E_z\Big|_{i,j+1}^{n} - E_z\Big|_{i,j}^{n}\right) + (1-\alpha_0)\left(E_z\Big|_{i+1,j+1}^{n} + E_z\Big|_{i-1,j+1}^{n} - E_z\Big|_{i+1,j}^{n} - E_z\Big|_{i-1,j}^{n}\right)\right) \tag{24}$$

$$H_y\Big|_{i+1/2,j}^{n+1/2} = H_y\Big|_{i+1/2,j}^{n-1/2} + \frac{\Delta t s_\omega(\Delta t)}{\mu s_k(\delta)}\left(\alpha_0\left(E_z\Big|_{i+1,j}^{n} - E_z\Big|_{i,j}^{n}\right) + (1-\alpha_0)\left(E_z\Big|_{i+1,j+1}^{n} + E_z\Big|_{i+1,j-1}^{n} - E_z\Big|_{i,j+1}^{n} - E_z\Big|_{i,j-1}^{n}\right)\right) \tag{25}$$

where $s_a(b) = 2\sin(ab/2)/a$ and

$$\alpha_0 = \frac{1}{2}(1+\gamma_0) \tag{26}$$

$$\gamma_0 = \frac{\cos(\tilde{k}'_x\delta)\cos(\tilde{k}'_y\delta) - \cos(\tilde{k}'\delta)}{1+\cos(\tilde{k}'_x\delta)\cos(\tilde{k}'_y\delta) - \cos(\tilde{k}'_x\delta) - cos(\tilde{k}'_y\delta)} \tag{27}$$

$$\tilde{k}'\delta = \frac{2\pi}{N'_\lambda} \tag{28}$$

$$\tilde{k}'_x\delta = \tilde{k}'\delta\cos(0.182\,03\pi) \tag{29}$$

$$\tilde{k}'_y\delta = \tilde{k}'\delta\sin(0.182\,03\pi) \tag{30}$$

and N'_λ is the discretization at which performance is optimum. Cole presented dispersion results in [11], but these were obtained by performing simulations and measuring errors. An analytic dispersion relation was not given. The parameter γ_0 was incorrect in [11] as was pointed out in [36]. Unfortunately, [36] contained a typographical error [37].

It can be seen that Cole's scheme uses an increased spatial stencil in the computation of the magnetic fields, but uses the same stencil as the standard Yee update equation in the computation of the electric field. As shown in Table I, this increased stencil roughly doubles the computational cost. In addition, the update equations have tunable coefficients, α_0 and γ_0, which serve to eliminate almost all dispersion errors at a given design frequency. However, Cole states that because the magnetic fields

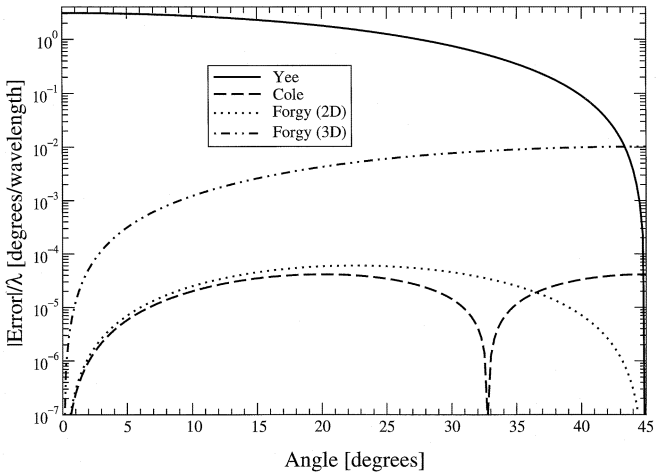

Fig. 5. Error versus propagation angle for the Yee, Forgy, and Cole schemes for a discretization of 10 CPW. The Forgy and Cole schemes have been optimized for 10 CPW. The curve labeled Forgy (3-D) was obtained using the α_0' of (38), while the Forgy (2-D) curve was obtained using the α_0' of (39).

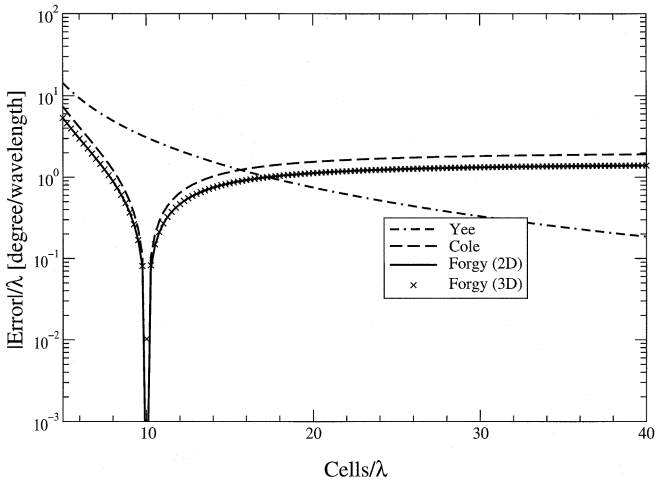

Fig. 6. Maximum error versus CPW for the Yee, Forgy, and and Cole schemes. Parameters for the higher-order schemes have been optimized for 10 CPW.

are computed first they contain an anisotropic error; thus, only the electric fields have high accuracy.

The dispersion relation for Cole's scheme is given by

$$\frac{\sin^2\left(\frac{\pi}{N_\lambda'}\right)}{\sin^2\left(\frac{\pi}{N_\lambda'}S\right)}\sin^2\left(\frac{\pi}{N_\lambda}S\right) = \left[\alpha_0+(1-\alpha_0)\cos\left(\frac{2\pi}{N_\lambda}\frac{\lambda}{\bar{\bar{\lambda}}}\sin\phi\right)\right]\sin^2\left(\frac{\pi}{N_\lambda}\frac{\lambda}{\bar{\bar{\lambda}}}\cos\phi\right) + \left[\alpha_0+(1-\alpha_0)\cos\left(\frac{2\pi}{N_\lambda}\frac{\lambda}{\bar{\bar{\lambda}}}\cos\phi\right)\right]\sin^2\left(\frac{\pi}{N_\lambda}\frac{\lambda}{\bar{\bar{\lambda}}}\sin\phi\right). \tag{31}$$

Fig. 5 shows the error versus propagation angle when the algorithm is optimized at 10 CPW. Note that the dispersion error is small over all angles and, thus, we consider this scheme to be "highly isotropic" (i.e., highly isotropic does not imply the error is nearly constant but rather it is consistently small). Fig. 6 shows the maximum error versus the discretization, again optimized at 10 CPW. Note the deep null in the dispersion error at the design frequency. This null is fairly narrowband, as indicated by the steep rise in the error at discretizations away from the design frequency.

Cole has also outlined a procedure to ensure negligible dispersion at the design frequency in three dimensions. Since the procedure is similar to the 2-D case, the dispersion error properties in 3-D will be similar to those obtained here in three dimensions.

VIII. Forgy's Isotropic FDTD Algorithm

Although starting with a different approach than Cole, Forgy developed an FDTD algorithm that has dispersion properties similar to Cole's scheme [12]–[14]. Forgy recognized that the dispersion errors of the Yee staggered grid and the Bi collocated grid were complimentary—the angles where the Yee algorithm has minimum dispersion are where the Bi algorithm has maximum dispersion, and vice versa. By using a simple linear combination (one-third Bi, two-thirds Yee) of the two schemes, he was able to develop an algorithm which was isotropic to fourth order. He also determined he could obtain a further reduction in the dispersion errors by 1) setting the error along the coordinate diagonals equal to the error along the main axis and 2) setting the error along the main axis equal to zero. By doing this, Forgy produced an algorithm that has almost no dispersion at a given design frequency. The resulting Forgy FDTD update equations are given by

$$\begin{aligned} E_z\Big|_{i,j}^{n+1} = E_z\Big|_{i,j}^{n} &+ \left(\frac{\alpha_0}{2}+\alpha_1\right)\frac{\Delta t}{\alpha_2\epsilon\delta}\left(H_y\Big|_{i+1/2,j}^{n+1/2} - H_y\Big|_{i-1/2,j}^{n+1/2} - H_x\Big|_{i,j+1/2}^{n+1/2} + H_x\Big|_{i,j-1/2}^{n+1/2}\right) \\ &+ \frac{\alpha_0}{2}\frac{\Delta t}{\alpha_2\epsilon\delta}\left(H_y\Big|_{i+1/2,j+1}^{n+1/2} + H_y\Big|_{i+1/2,j-1}^{n+1/2} - H_y\Big|_{i-1/2,j+1}^{n+1/2} - H_y\Big|_{i-1/2,j-1}^{n+1/2}\right. \\ &\left. - H_x\Big|_{i+1,j+1/2}^{n+1/2} - H_x\Big|_{i-1,j+1/2}^{n+1/2} + H_x\Big|_{i+1,j-1/2}^{n+1/2} + H_x\Big|_{i-1,j-1/2}^{n+1/2}\right) \end{aligned} \tag{32}$$

$$H_x\Big|_{i,j+1/2}^{n+1/2} = H_x\Big|_{i,j+1/2}^{n-1/2} - \frac{\Delta t}{\alpha_2\mu\delta}\left(E_z\Big|_{i,j+1}^{n} - E_z\Big|_{i,j}^{n}\right) \tag{33}$$

$$H_y\Big|_{i+1/2,j}^{n+1/2} = H_y\Big|_{i+1/2,j}^{n-1/2} + \frac{\Delta t}{\alpha_2\mu\delta}\left(E_z\Big|_{i+1,j}^{n} - E_z\Big|_{i,j}^{n}\right) \tag{34}$$

where α_0, α_1, and α_2 are given by

$$\alpha_0 = \frac{\pi\alpha_0'}{N_\lambda'\sin\left(\frac{\pi}{N_\lambda'}\right)} \tag{35}$$

$$\alpha_1 = \frac{\pi(1-\alpha_0')}{N_\lambda'\sin\left(\frac{\pi}{N_\lambda'}\right)} \tag{36}$$

$$\alpha_2 = \frac{\pi S}{N_\lambda'\sin\left(\frac{\pi S}{N_\lambda'}\right)}. \tag{37}$$

In [13], α_0' is given as

$$\alpha_0' = \frac{\sqrt{3}\sin\left(\frac{\pi}{N_\lambda'\sqrt{3}}\right) - \sin\left(\frac{\pi}{N_\lambda'}\right)}{\sqrt{3}\sin^3\left(\frac{\pi}{N_\lambda'\sqrt{3}}\right)}. \tag{38}$$

This value ensures that the error for propagation along the grid axes is the same as for propagation along the 3-D grid diagonals (i.e., the diagonals that connect opposite corners of a cube). However, since we are considering only 2-D propagation, a different value of α_0' should be used to ensure that the error for propagation along the grid axes is the same as that for propagation along the 2-D grid diagonals. This value can be derived by following the procedure outlined in [13, Sec. 6.1] with the wavenumber set to zero along one of the grid axes. The resulting 2-D value of α_0' is

$$\alpha_0' = \frac{2\sin^2\left(\frac{\pi}{N_\lambda'\sqrt{2}}\right) - \sin^2\left(\frac{\pi}{N_\lambda'}\right)}{2\sin^4\left(\frac{\pi}{N_\lambda'\sqrt{2}}\right)}. \tag{39}$$

As will be shown, both the 2-D and 3-D versions of α_0' yield similar results except at the design frequency.

It is interesting to note that in the 2-D case, this scheme uses the same spatial stencil as the Yee scheme in computation of the magnetic fields, but uses a larger stencil in the computation of the electric field. Thus, the stencils for the electric and magnetic fields are complimentary in nature to that of Cole's scheme. In addition, it can be seen that like the Cole scheme, there are coefficients of the form $\sin(x)/x$ in the update equations. As indicated in Table I, the Forgy scheme also uses slightly fewer floating point operations than the Cole scheme, while having a slightly larger optimal Courant number.

The dispersion relation is given by

$$\begin{aligned}
&\frac{\alpha_2^2}{S^2}\sin^2\left(\frac{\pi}{N_\lambda}S\right)\\
&=(\alpha_0+\alpha_1)\left(\alpha_0\cos^2\left(\frac{\pi}{N_\lambda}\frac{\lambda}{\tilde{\lambda}}\sin\phi\right)+\alpha_1\right)\\
&\quad\times\sin^2\left(\frac{\pi}{N_\lambda}\frac{\lambda}{\tilde{\lambda}}\cos\phi\right)\\
&\quad+(\alpha_0+\alpha_1)\left(\alpha_0\cos^2\left(\frac{\pi}{N_\lambda}\frac{\lambda}{\tilde{\lambda}}\cos\phi\right)+\alpha_1\right)\\
&\quad\times\sin^2\left(\frac{\pi}{N_\lambda}\frac{\lambda}{\tilde{\lambda}}\sin\phi\right).
\end{aligned} \tag{40}$$

Figs. 5 and 6 show the dispersion errors versus propagation angle and discretization when optimized at 10 CPW, respectively. As can be seen from Fig. 5, when using the 2-D value of α_0' the dispersion error is highly isotropic, with no dispersion at 0°, 45°, and integer multiples of 45°. Using the 3-D value of α_0' yields zero error only along the grid axes and yields a maximum error which is more than two orders of magnitude larger than that obtained using the 2-D value. This figure indicates that a substantial improvement can be realized at the design frequency in a 2-D simulation by using the α_0' given in (39) instead of the one given in (38). However, away from the design frequency, the difference in errors is almost imperceivable as shown in Fig. 6. In Fig. 6, the 2-D Forgy scheme is plotted with a solid line while the 3-D scheme is plotted using Xs. The 3-D results are almost identical to the 2-D ones except at the design frequency of 10 CPW where a single X can be seen hovering in the null.

In general, the behavior of the error versus discretization is similar to Cole's algorithm, showing a deep null at the design frequency and a steep rise at discretizations away from this frequency. At the design frequency, the maximum error of the Cole scheme is approximately one-fifth as large as the M(2,4) scheme (which has the smallest maximum of all the (2,4) methods). The maximum error of the 2-D Forgy scheme is approximately one-third that of the M(2,4) scheme. One major advantage of the Forgy scheme over the Cole scheme is that, unlike Cole's scheme, Forgy's scheme is accurate in both the electric and magnetic fields.

Since the Forgy algorithm ensures the errors along the coordinate diagonals and axes are zero, the dispersion behavior in three dimensions is similar to that of the 2-D case investigated here.

IX. MRTD Algorithm

In 1996, Krumpholz and Katehi developed a new approach to time-domain analysis, termed the MRTD approach [15]. They expanded the electric and magnetic field components in terms of scaling and wavelet basis functions with respect to space. Similar functions were used as testing functions in space. Pulse functions were used as both basis and testing functions in time.

The MRTD coefficients for the field expansions, when solely using scaling functions, are given by

$$\begin{aligned}
E_{z,\phi}\Big|_{i,j}^{n+1} =& E_{z,\phi}\Big|_{i,j}^{n} + \frac{\Delta t}{\epsilon\delta}\left(\sum_{i'=i-n_a}^{i+n_a-1} a(i')H_{y,\phi}\Big|_{i'-1/2,j}^{n+1/2}\right.\\
&\left.-\sum_{j'=j-n_a}^{j+n_a-1} a(j')H_{x,\phi}\Big|_{i,j'-1/2}^{n+1/2}\right)
\end{aligned} \tag{41}$$

$$\begin{aligned}
H_{x,\phi}\Big|_{i,j+1/2}^{n+1/2} =& H_{x,\phi}\Big|_{i,j+1/2}^{n-1/2}\\
&-\frac{\Delta t}{\mu\delta}\sum_{j'=j-n_a}^{j+n_a-1} a(j')E_{z,\phi}\Big|_{i,j'}^{n+1/2}
\end{aligned} \tag{42}$$

$$\begin{aligned}
H_{y,\phi}\Big|_{i+1/2,j}^{n+1/2} =& H_{y,\phi}\Big|_{i+1/2,j}^{n-1/2}\\
&+\frac{\Delta t}{\mu\delta}\sum_{i'=i-n_a}^{i+n_a-1} a(i')E_{z,\phi}\Big|_{i',j}^{n+1/2}
\end{aligned} \tag{43}$$

where n_a is the size of the computational stencil, and the coefficients $a(i')$ and $a(j')$ depend on the choice of scaling functions used. The electric and magnetic fields are obtained from these field expansions. Equations (41)–(43) show that the amount of computation per update is directly related to the choice of the scaling function used in the field expansion. Scaling functions with large support use large spatial stencils and require extensive computation, while those with compact support require much less computation.

When only scaling functions are used (as opposed to using wavelets and scaling functions), the MRTD dispersion relation is given by

$$\frac{1}{S^2}\sin^2\left(\frac{\pi}{N_\lambda}S\right) = \left[D_x^\phi\left(\tilde{k}_x\delta\right)\right]^2 + \left[D_y^\phi\left(\tilde{k}_y\delta\right)\right]^2 \tag{44}$$

TABLE II
COEFFICIENTS USED IN THE UPDATE EQUATIONS FOR THE MRTD METHODS BASED ON B–L, DAUBECHIES, OR HAAR SCALING FUNCTIONS

	$a(i)$		
i	B-L	Daubechies	Haar
0	1.2918462	1.22916661202745	1.00
1	-0.1560761	-0.09374997764764	
2	0.0596391	0.01041666418309	
3	-0.0293099		
4	0.0153716		
5	-0.0081892		
6	0.0043788		
7	-0.0023433		
8	0.0012542		

where

$$D_x^{\phi}\left(\tilde{k}_x\delta\right) = \sum_{i=0}^{n_a} a(i)\sin\left(\frac{\pi}{N_\lambda}\frac{\lambda}{\tilde{\lambda}}\left(i+\frac{1}{2}\right)\cos\phi\right) \quad (45)$$

$$D_y^{\phi}\left(\tilde{k}_y\delta\right) = \sum_{i=0}^{n_a} a(i)\sin\left(\frac{\pi}{N_\lambda}\frac{\lambda}{\tilde{\lambda}}\left(i+\frac{1}{2}\right)\sin\phi\right). \quad (46)$$

A. Krumpholz and Katehi's MRTD Using Battle–Lemarie Scaling Functions

Although many possibilities exist for the choice of the wavelet or scaling functions, Krumpholz and Katehi originally developed their MRTD scheme using cubic spline Battle–Lemarie scaling functions and wavelet functions [15]. When performing a dispersion analysis on the Battle–Lemarie wavelet functions, the authors determined that the use of these wavelet functions lead to spurious modes. They, therefore, concentrated their efforts on the Battle–Lemarie scaling functions.

Krumpholz and Katehi noted that although the Battle–Lemarie scaling functions have infinite support, the functions have exponential decay and, thus, can be approximated by functions with compact support. The use of 9–12 coefficients have been reported. Using nine coefficients results in Battle–Lemarie scaling functions with 18 terms. This was the case considered in Krumpholz and Katehi's original paper and also used here. The $a(i)$ for the Battle–Lemarie scaling functions are given in the first column of Table II. Fig. 7 shows the dispersion error of the MRTD scheme using the Battle–Lemarie scaling functions versus propagation angle when optimized at 10 CPW. This curve used the optimal Courant number for 10 CPW of 0.2575. The maximum dispersion error versus CPW is shown in Fig. 8. The use of Battle–Lemarie scaling functions in the MRTD method results in good dispersion behavior for high frequencies.

The dispersion properties of the 3-D MRTD scheme using Battle–Lemarie scaling functions was presented in [38], where it was shown that the 3-D dispersion behavior is similar to that of the 2-D case.

B. Cheong et al.'s MRTD Using Daubechies Scaling Functions

Motivated by a desire to increase the localization of the field components, Cheong *et al.* developed a scheme they called the Wavelet–Galerkin MRTD method, which is based on compactly supported Daubechies scaling functions [21]. By using the Daubechies scaling functions, the authors were able to reduce the amount of computation required by the Battle–Lemarie scaling functions. This is because the Daubechies scaling functions requires only three coefficients, rather than the 9–12 required by the Battle–Lemarie scaling functions. The $a(i)$ coefficients used in (45) and (46) are given in the second column of Table II. As shown in Table I, the FLOPs per cell per time step is 48 for the Daubechies scaling functions in contrast to 144 FLOPs for the Battle–Lemarie scaling functions.

A plot of the dispersion error versus propagation angle when optimized at 10 CPW is given in Fig. 7. An optimal Courant number of 0.033 was used to generate this curve. It can be seen from Fig. 7 that the Daubechies MRTD scheme has more error than the B–L MRTD scheme. The maximum dispersion error versus CPW is shown in Fig. 8. It is interesting to note that the Daubechies MRTD is much more wideband than the B–L MRTD. It is also interesting that the Daubechies MRTD scheme behaves as third order, which greatly reduces the dispersion errors at high discretizations.

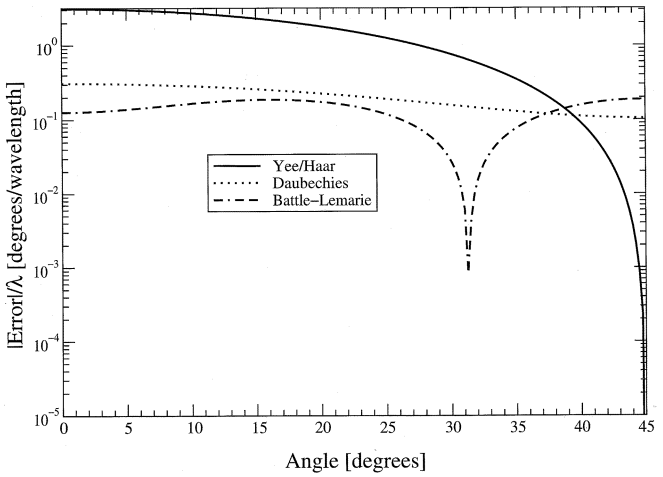

Fig. 7. Error versus propagation angle for the MRTD schemes employing either Haar, Battle–Lemarie, or Daubechies scaling functions. Parameters have been optimized for 10 CPW. The Haar results are identical to those of the Yee scheme.

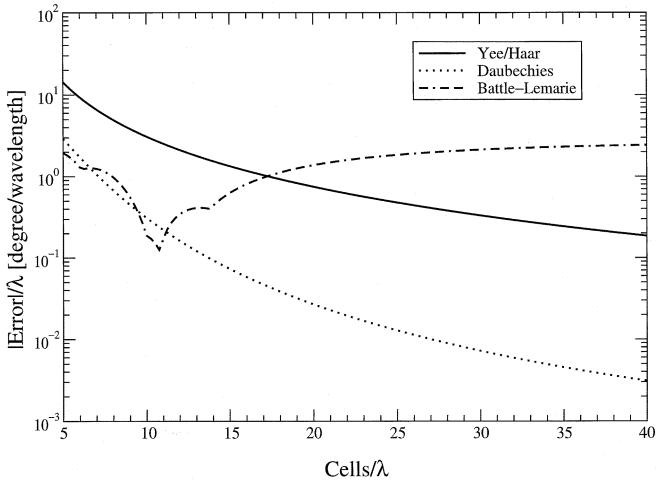

Fig. 8. Maximum error versus CPW for the MRTD schemes employing either Haar, Battle–Lemarie, or Daubechies scaling functions. Parameters have been optimized for 10 CPW. The Haar results are identical to those of the Yee scheme.

The dispersion errors of the Daubechies MRTD scheme in three dimensions is similar to the 2-D errors presented. It is noted that the dispersion properties of the Daubechies MRTD using higher order moments was recently published in [24].

C. MRTD Using Haar Scaling Functions

In order to avoid the undesirable noncompact support of the B–L scaling functions, Goverdhanam *et al*. [16] and Fujii and Hoefer [19], [20] independently explored the use of Haar scaling functions. As shown by the $a(i)$ coefficients given in the third column of Table II, use of the Haar scaling functions results in very compact support [39]. These coefficients are, in fact, the coefficients for the standard Yee update equations. Thus, the dispersion relation of the MRTD method using Haar scaling functions is identical to that of the Yee algorithm. Its dispersion properties are also shown in Figs. 7 and 8 for comparison against the other MRTD schemes.

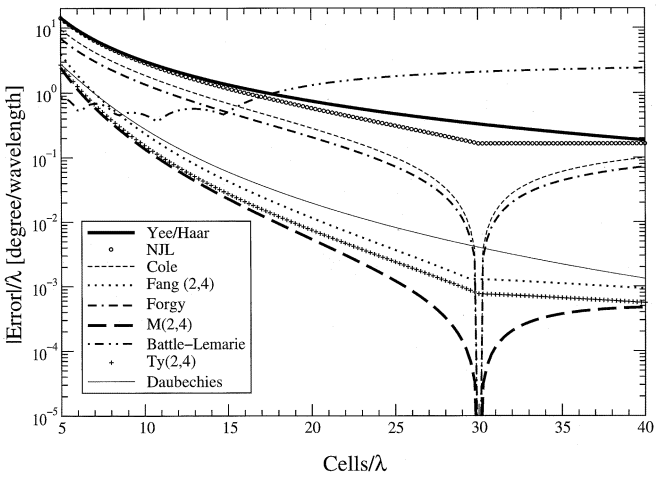

Fig. 9. Maximum error versus CPW when the methods have been optimized for 30 CPW.

X. Comparison of FDTD Algorithms

In this section, we summarize the computation involved and the numerical dispersion of all the previously described FDTD algorithms. Column 2 of Table I gives the number of floating point operations to update each cell (three fields) per time step. It can be seen that the simple NJL scheme requires no additional operations over the Yee algorithm. Most of the other schemes require roughly two to three times as many operations. Excluding the Haar-based MRTD scheme, the MRTD schemes require substantially more computation than the Yee algorithm due to their large spatial stencils. The MRTD method using Daubechies scaling functions requires over four times as many operations as the Yee scheme, while MRTD using Battle–Lemarie scaling functions requires roughly 13 times as many. Column 3 of Table I gives the optimum Courant number for each scheme at a resolution of 10 CPW, while column 4 gives the optimum Courant number at a resolution of 30 CPW. As can be seen from Table I, the Forgy algorithm permits the largest time step, which translates into the fewest number of updates for a simulation of a given duration. The Battle–Lemarie MRTD, Daubechies MRTD, Fang(2,4), and Ty(2,4) approaches all require the smallest time steps and hence the greatest number of updates.

Figs. 2, 4, 6, and 8 show the maximum dispersion error versus grid spacing when each scheme was optimized at a design frequency of 10 cells per wavelength. These figures, along with Figs. 3 and 5, show that the Cole and 2-D Forgy optimized dispersion schemes produce the lowest levels of dispersion at the design frequency, but have higher errors than most of the other schemes away from the design frequency. The Battle–Lemarie MRTD scheme behaves well for high frequencies but has the greatest error at low frequencies. The Cole, Forgy, Battle–Lemarie MRTD, and NJL schemes all actually have worse dispersion errors at the lower frequencies than the Yee algorithm. However, the conclusions which one draws from these figures can be altered by changing the frequency at which optimization occurs. For example, Fig. 9 shows the maximum dispersion versus grid spacing for each scheme when evaluated at a resolution of 30 CPW and an optimal Courant number at this resolution (see column 4 of Table I). As in the 10 CPW case, the Cole and 2-D Forgy algorithms have deep nulls at the design frequency (results for the 3-D Forgy scheme are not shown). Similar to these schemes, the M(2,4) algorithm has a deep null, but it also possesses the best dispersion behavior over nearly all frequencies. The Fang(2,4), Ty(2,4), and Daubechies MRTD have excellent dispersion properties over all frequencies. In fact, at all frequencies in the plot, every scheme except for MRTD using B–L scaling functions now behaves better than the Yee scheme. As in the 10 CPW case, the B–L MRTD scheme performs better than the Yee scheme only at higher frequencies.

Table III summarizes the advantages and disadvantages of each of the FDTD schemes. Clearly, there are advantages and disadvantages to each, and, depending on whether narrowband or wideband results are desired, one scheme may be preferred over another. Table III is based solely upon the dispersive properties of the schemes in two dimensions. We have not attempted to characterize other important issues such as the ability of the schemes to model general inhomogeneous material or the suitability of the scheme for full 3-D modeling.

XI. Conclusion

We have analyzed the 2-D dispersion properties of several new low-dispersion FDTD algorithms. Almost all provide substantial improvement in the reduction of dispersion errors compared with the classical Yee algorithm. In almost all cases, these improvements add additional computational cost to the algorithm. In addition, for several of the algorithms, a much smaller Courant number must be used to obtain the added benefit of highly reduced dispersion. Depending on the particular application, one of the low-dispersion FDTD schemes may be preferred over another. Although a 3-D dispersion analysis was not presented, for most of the algorithms discussed here similar dispersion behavior occurs in the 3-D case.

TABLE III
ADVANTAGES AND DISADVANTAGES

Scheme		Advantages	Disadvantages
NJL		simple to implement no added computation no added storage	only minor improvement anisotropic
Fang(2,4)		good wideband performance	small Courant number not very isotropic
M(2,4)		good wideband performance good narrowband performance nearly isotropic	large stencil not as isotropic as Forgy or Cole
Ty(2,4)		good wideband performance	complicated (matrix inversion) small Courant number not very isotropic
Cole		excellent narrowband performance highly isotropic large Courant number	not as wideband as many other schemes accurate only in electric fields
Forgy		excellent narrowband performance highly isotropic largest Courant number	not as wideband as many other schemes
MRTD	Battle-Lemarie	good performance at high freq.	extremely large stencil extremely large FLOP count not very isotropic small Courant number
	Daubechies	good wideband performance third-order behavior	large stencil large FLOP count not very isotropic very small Courant number
	Haar	simplest MRTD scheme	same dispersion as Yee

ACKNOWLEDGMENT

The authors would like to thank E. Forgy of the University of Illinois, Urbana-Champaign, for many helpful comments concerning the implementation and analysis of the algorithms considered here. We further thank M. Fujii, J. Cole, and K. Goverdhanam for providing useful information.

REFERENCES

[1] K. L. Shlager, J. G. Maloney, S. L. Ray, and A. F. Peterson, "Relative accuracy of several finite-difference time-domain methods in two and three dimensions," *IEEE Trans. Antennas Propagat.*, vol. 41, pp. 1732–1737, Dec. 1993.

[2] K. S. Yee, "Numerical solution of initial boundary value problems involving Maxwell's equations in isotropic media," *IEEE Trans. Antennas Propagat.*, vol. 14, pp. 302–307, Mar. 1966.

[3] J. Fang, "Time domain finite difference computation for Maxwell's equations," Ph.D. dissertation, Univ. California, Berkeley, CA, 1989.

[4] Z. Bi, K. Wu, C. Wu, and J. Litva, "A new finite-difference time-domain algorithm for solving Maxwell's equations," *IEEE Microwave Guided Wave Lett.*, vol. 1, pp. 382–384, Dec. 1991.

[5] Z. Chen, M. M. Ney, and W. J. R. Hoefer, "A new finite-difference time-domain formulation and its equivalence with the TLM symmetrical condensed node," *IEEE Trans. Microwave Theory Tech.*, vol. 39, pp. 2160–2169, Dec. 1991.

[6] J. W. Nehrbass, J. O. Jevtić, and R. Lee, "Reducing the phase error for finite-difference methods without increasing the order," *IEEE Trans. Antennas Propagat.*, vol. 46, pp. 1194–1201, Aug. 1998.

[7] A. Taflove, *Computational Electrodynamics: The Finite-Difference Time-Domain Method*. Norwood, MA: Artech House, 1995.

[8] M. F. Hadi and M. Piket-May, "A modified FDTD (2,4) scheme for modeling electrically large structures with high-phase accuracy," *IEEE Trans. Antennas Propagat.*, vol. 45, pp. 254–264, Feb. 1997.

[9] E. Turkel and A. Yefet, "Fourth order method for Maxwell's equations on a staggered mesh," in *Proc. IEEE Antennas and Propagat. Soc. Int. Symp.*, vol. 4, Montréal, QC, Canada, July 1997, pp. 2156–2159.

[10] E. Turkel, "High-order methods," in *Advances in Computational Electrodynamics: The Finite-Difference Time-Domain Method*, A. Taflove, Ed. Norwood, MA: Artech House, 1998, ch. 2, pp. 63–110.

[11] J. B. Cole, "A high-accuracy realization of the Yee algorithm using nonstandard finite differences," *IEEE Trans. Microwave Theory Tech.*, vol. 45, pp. 991–996, June 1997.

[12] E. A. Forgy and W. C. Chew, "An efficient FDTD algorithm with isotropic numerical dispersion on an overlapped lattice," in *Proc. IEEE Antennas and Propagat. Soc. Int. Symp.*, vol. 4, Atlanta, GA, June 1998, pp. 1812–1815.

[13] E. A. Forgy, "A time-domain method for computational electromagnetics with isotropic numerical dispersion on an overlapped latice," Master's thesis, Univ. Illinois, Urbana-Champaign, 1998.

[14] E. A. Forgy and W. C. Chew, "A time domain method with isotropic dispersion and increased stability on an overlapped lattice," *IEEE Trans. Antennas Propagat.*, vol. 50, pp. 983–996, July 2002.

[15] M. Krumpholz and L. P. B. Katehi, "MRTD: New time-domain schemes based on multiresolution analysis," *IEEE Trans. Microwave Theory Tech.*, vol. 44, pp. 555–571, Apr. 1996.

[16] K. Goverdhanam, E. Tentzeris, M. Krumpholz, and L. P. B. Katehi, "An FDTD multigrid based on multiresolution analysis," in *IEEE Antennas and Propagat. Soc. Int. Symp.*, vol. 1, Baltimore, MD, July 1996, pp. 352–355.

[17] K. Goverdhanam, L. P. B. Katehi, and A. Cangellaris, "Applications of multiresolution based FDTD multigrid," in *Proc. IEEE MTT-S Int. Microwave Symp.*, vol. 1, Denver, CO, June 1997, pp. 333–336.

[18] K. Goverdhanam and L. P. B. Katehi, "Applications of Haar wavelet based MRTD scheme in the characterization of 3D microwave circuits," in *Proc. IEEE MTT-S Int. Microwave Symp.*, vol. 4, Anaheim, CA, June 1999, pp. 1475–1478.

[19] M. Fujii and W. J. R. Hoefer, "A three-dimensional Haar-wavelet-based multiresolution analysis similar to the FDTD method—Derivation and application," *IEEE Trans. Microwave Theory Tech.*, vol. 46, pp. 2463–2475, Dec. 1998.

[20] ——, "Numerical dispersion in Haar-wavelet based MRTD scheme—Comparison between analytical and numerical results," in *Proc. 15th Annu. Rev. Progress in Applied Computational Electromagnetics*, Monterey, CA, Mar. 1999, pp. 602–607.

[21] Y. W. Cheong, Y. M. Lee, K. H. Ra, J. G. Kang, and C. C. Shin, "Wavelet-Galerkin scheme of time-dependent inhomogeneous electromagnetic problems," *IEEE Microwave Guided Wave Lett.*, vol. 9, pp. 297–299, Aug. 1999.

[22] S. R. Omick and S. P. Castillo, "A new finite-difference time-domain algorithm for the accurate modeling of wide-band electromagnetic phenomena," *IEEE Trans. Electromagn. Compat.*, vol. 35, pp. 215–222, May 1993.

[23] Q. H. Liu, "The PSTD algorithm: A time-domain method requiring only two cells per wavelength," *Microw. Opt. Technol. Lett.*, vol. 15, no. 3, pp. 158–165, 1997.
[24] M. Fujii and W. J. R. Hoefer, "Dispersion of time domain wavelet Galerkin method based on Daubechies' compactly supported scaling functions with three and four vanishing moments," *IEEE Microwave Guided Wave Lett.*, vol. 4, pp. 125–127, Apr. 2000.
[25] ——, "Time-domain wavelet Galerkin modeling of two-dimensional electrically large dielectric waveguides," *IEEE Trans. Microwave Theory Tech.*, vol. 49, pp. 886–892, May 2001.
[26] T. Dogaru and L. Carin, "Multiresolution time-domain using CDF biorthogonal wavelets," *IEEE Trans. Microwave Theory Techn.*, vol. 49, pp. 902–912, May 2001.
[27] A. Taflove, "Review of the formulation and applications of the finite-difference time-domain method for numerical modeling of electromagnetic wave interactions with arbitrary structures," *Wave Motion*, vol. 10, no. 6, pp. 547–582, 1988.
[28] J. B. Schneider and C. L. Wagner, "FDTD dispersion revisited: Faster-than-light propagation," *IEEE Microwave Guided Wave Lett.*, vol. 9, pp. 54–56, Feb. 1999.
[29] J. L. Young, "The design of high-order, leap-frog integrators for Maxwell's equations," in *Proc. IEEE Antennas and Propagat. Soc. Int. Symp.*, vol. 1, Orlando, FL, July 1999, pp. 176–179.
[30] A. Yefet and P. G. Petropoulos, "A Non-dissipative staggered fourth-order accurate explicit finite difference scheme for the time-domain Maxwell's equations," Inst. Comput. Applicat. Sci. Eng., Tech. Rep. NASA/CR-1999–209 514, 1999.
[31] ——, "A staggered fourth-order accurate explicit finite difference scheme for the time-domain Maxwell's equations," *J. Computat. Phys.*, vol. 168, no. 2, pp. 286–315, 2001.
[32] K.-P. Hwang and A. C. Cangellaris, "Numerical boundary conditions at material interfaces for high-order FDTD simulations," in *Proc. USNC/URSI*, Boston, MA, July 2001, p. 251.
[33] G. J. Haussmann, "A dispersion optimized three-dimensional finite-difference time-domain method for electromagnetic analysis," Ph.D. dissertation, Univ. Colorado, Boulder, 1998.
[34] H. E. Abd El-Raouf, E. A. El-Diwani, A. E.-H. Ammar, and F. M. El-Hefnawi, "A modified 3D fourth order FDTD algorithm $M3d_{24}$ for improving phase accuracy with low resolution," in *Proc. IEEE Antennas and Propagat. Soc. Int. Symp.*, vol. 1, Orlando, FL, July 1999, pp. 196–199.
[35] J. L. Young, D. Gaitonde, and J. S. Shang, "Toward the construction of a fourth-order difference scheme for transient EM wave simulation: Staggered grid approach," *IEEE Trans. Antennas Propagat.*, vol. 45, pp. 1573–1580, Nov. 1997.
[36] J. B. Cole, "A high-accuracy realization of the Yee algorithm using non-standard finite differences," *IEEE Trans. Microwave Theory Tech.*, vol. 46, p. 202, Feb. 1998.
[37] J. Cole, private communication, Sept. 1998.
[38] K. L. Shlager and J. B. Schneider, "Analysis of the dispersion properties of the multiresolution time-domain (MRTD) scheme," in *Proc. IEEE Antennas and Propagat. Soc. Int. Symp.*, vol. 4, Montréal, QC, Canada, July 1997, pp. 2144–2147.
[39] M Fujii, private communication, Sept. 1999.

Kurt L. Shlager (S'81–M'88–S'91–M'96–SM'02) received the B.S. degree in electrical engineering from Southeastern Massachusetts University (now UMass at Dartmouth), North Dartmouth, the M.S. degree in electrical engineering from Tufts University, Medford, MA, and the Ph.D. degree in electrical engineering from the Georgia Institute of Technology, Atlanta, in 1985, 1987, and 1995, respectively.

He has been with GTE Government Systems, Westborough, MA, TRW Space and Electronics Group, Redondo Beach, CA, Space Systems Loral, Palo Alto, CA, and Lockheed-Martin Space Systems Company, Sunnyvale, CA, where he is currently a Staff Engineer. His research interests include the FDTD method, electromagnetic scattering, and antenna analysis and design. He coauthored the chapter "A survey of the finite-difference time-domain literature" in *Advances in Computational Electrodynamics: The Finite-Difference Time-Domain Method* (Norwood, MA: Artech House, 1998). He has published approximately 25 refereed journal and conference papers.

John B. Schneider received the B.S. degree in electrical engineering from Tulane University, New Orleans, LA, and the M.S. and Ph.D. degrees in electrical engineering from the University of Washington, Pullman.

He is currently an Associate Professor with the School of Electrical Engineering and Computer Science, Washington State University, as well as the school's Associate Director. His research interests include the use of computational methods to analyze acoustic, elastic, and electromagnetic wave propagation.